EUROSTEEL 2011, August 31 - September 2, 2011, Budapest, Hungary

RESIDUAL STRESS CALCULATION IN COLD-ROLLED STEEL TUBES WITH FEA: VALIDATION OF THE STRAIN EVOLUTION

Maarten De Strycker [a], Wim Van Paepegem [b], Dimitri Debruyne [c,a] and Luc Schueremans [d]

[a] KaHo St.-Lieven associatie KULeuven, MeM2P, Belgium
[b] Ghent University, Dept. of Materials Science and Engineering, Belgium
[c] KULeuven, Dept. MTM, Belgium
[d] KULeuven, Dept. of Civil Engineering, Belgium

INTRODUCTION

Residual stresses affect the application of steel tubes in many ways and their magnitude and distribution are of particular interest. Residual stresses in cold-rolled steel tubes are inherent to the production process: first a flat steel plate (not necessary initially stress free) is rolled into a circular cross-section and then both edges of the plate are welded together to obtain a closed cross-section. The first step involves non-homogeneous plastic deformations and the second imposes a non-uniform heating and cooling cycle. The focus in this research is on the residual stresses due to the welding step.

To discover the residual stresses in the tubes under consideration, a finite element analysis (FEA) is made. With FEA all the residual stress components after welding in the whole tube are revealed. The result is however dependent on the input for the simulation: thermo-mechanical temperature-dependent material properties, thermal load definition, thermal and mechanical boundary conditions. Validation of the FEA results is therefore important.

Welding simulations are usually split up into two separate analyses: first the temperature evolution in the welded construction is calculated from the heat input and next, starting from the temperature field, the stress and strain development due to the temperature cycle is calculated in a mechanical analysis. The thermal field used for the mechanical simulation, can be validated by measuring the transient temperatures in the construction. The mechanical analysis, in which more material parameters are introduced and more assumptions are made, induces a more complicated stress-strain validation.

Lindgren [1] gives an extensive overview of papers describing validation methods for the mechanical analysis. These include residual strain measurements using hole-drilling techniques, X-ray techniques, or neutron diffraction measurements; transient strains have also been measured in some cases using high-temperature strain gauges. The mentioned methods have some drawbacks: only in a restricted number of points the deformations and strains are available (in the case of displacement sensors and strain gauges), temperature compensation is needed (for strain gauges), only the final stress-strain state is known (for residual stress measurements), the part is lost (destructive residual stress measuring methods), the method requires a complex setup (laser interferometry, X-ray diffraction and neutron diffraction residual stress measurements), which is sensitive to vibrations, differences in the density of the air between the measurement device and the welded object (laser interferometry).

In the current research, the numerically predicted deformation is tested against the experimentally measured one. This can be done with the Digital Image Correlation (DIC) technique. Compared to other measuring methods used in welded structures, DIC has the major advantage that it is a contactless method; that it can discover the deformations over a significant portion of the surface when a work piece is welded, even in zones that heat up to 600°C and without the need for thermal compensation on the measured strains. It has, however, the drawback that it is conventionally not judged suited for small strains that occur in the welding case under consideration here. As it is not common to measure deformations in a welding process with DIC, the results are compared to strains measured with electrical strain gauges (SG). Both methods measure deformations on a different basis and are independent. First it is shown that both techniques yield similar results to

prove that DIC can be used as a validation tool for welding simulations. Next, the experimental results are compared with the FEA results.

1 EXPERIMENTAL DATA

1.1 Setup

The experimental setup is a modified version of the actual industrial production process. In the laboratory, the tube is kept static and the welding torch is moved above it by a robot. To avoid overexposure on the images taken during the welding, the blazing light of the GTAW weld beam is shielded by a tin foil wrapped around the cup of the torch. The use of a robot assures controlled welding conditions: the distance between the tube and the electrode is invariably 2mm along the weld bead and the welding speed is 2mm/s. The length of the weld bead is confined to 30cm, this length yields a stress-strain state that is uniform over a sufficiently long part of the tube. To avoid complications of applying closing forces (which would hamper the making of the images for DIC), the welding experiments start from an already finished tube, i.e. a tube that was rolled and welded before.

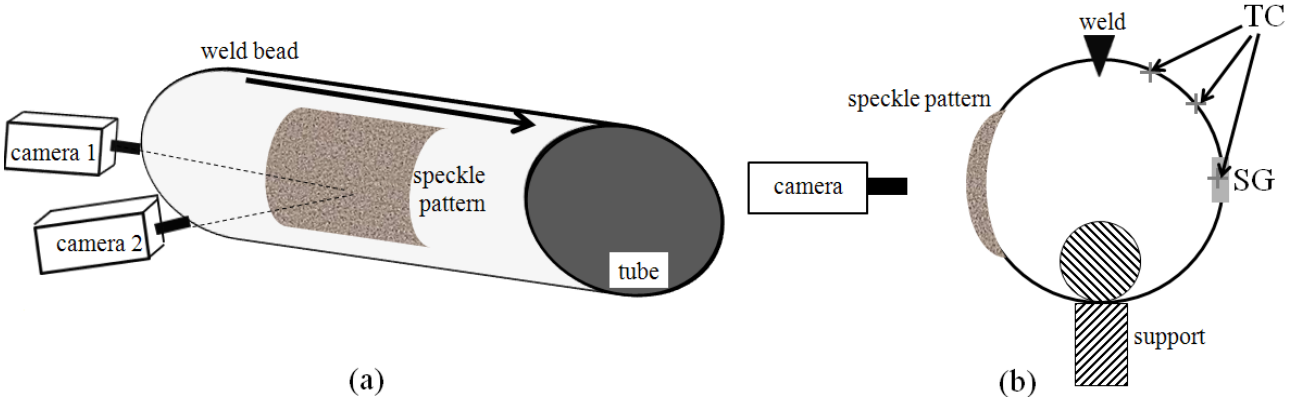

Fig.1. Sketch of the setup of the tube with the DIC cameras and indication of the strain gauge (SG) and thermocouple (TC) position. Thermocouples are positioned around the strain gauges.

In Fig.1 the setup is sketched: one side of the tube is instrumented for the DIC measurements (a speckle pattern that is filmed by two cameras), the other side for temperature measurements with thermocouples (TC) and strain gauge (SG) measurements. As the strain gauges are positioned symmetrically to the speckle pattern with regard to the weld bead and the support, the deformations measured with both techniques should be comparable.

1.2 Tubes under consideration

The tubes under consideration are stainless steel (RVS304) tubes with a diameter of 60mm, a wall thickness of 1.5mm and are 40cm long. It was shown in simulations that residual stresses have an influence on the measured strain evolution during the welding. As the actual residual stresses are the subject of the research project, these are not known at the moment. Therefore, the tubes as delivered from the manufacturer are annealed for 11 days on 400°C to remove the residual stresses due to the rolling and welding from the production process.

1.3 Strain gauge measurement

As the steel under the strain gauge heats during the welding, spurious thermal strains (ε_s) need to be compensated. Also the difference between the thermal expansion coefficient between the steel (α_m) and the carrier of the strain gauge (α_{SG}) needs to be compensated by taking into account the temperature difference $\Delta\theta$. The thermal strain (ε_{th}) measured in the material is calculated from the measured strain (ε_a) as follows:

$$\varepsilon_{th} = \alpha_m \,.\, \Delta\theta = \varepsilon_a - \varepsilon_s + \alpha_{SG} \,.\, \Delta\theta$$

So the results are depending on the accuracy of the temperature measurement. TC3 (see Fig.2(a)) is positioned in between the two strain gauges. This curve gives an indication of the temperature cycle

that the strain gauge is subjected to during the welding. The result of this procedure for the strain gauge in hoop direction is given in Fig.2(b).
In total three tubes were welded under these conditions. All measurements yield very similar results.

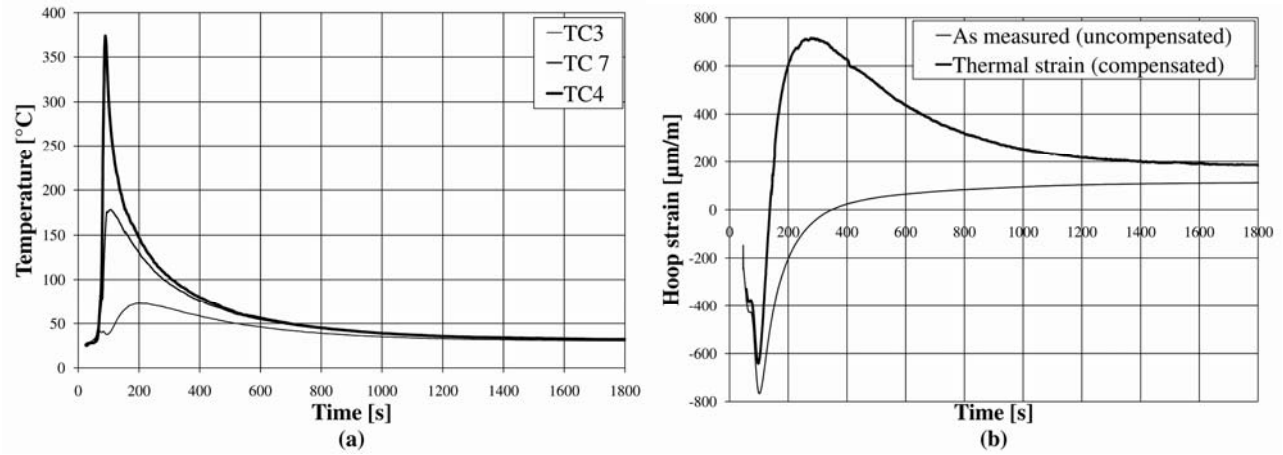

Fig. 2. Experimentally obtained results: (a) selection of temperature measurements for different thermocouples (TC) and (b) strain in hoop direction: the raw data (as measured) and the thermal strain that is inferred from the measurement.

1.4 DIC measurement

The digital image correlation technique (DIC) is a full-field deformation measurement technique. In this method, the deformations of the object under investigation are analysed with the aid of a speckle pattern attached to the surface of the object. This speckle pattern consists of a uniform white background with a random pattern of black speckles on it. The deformation of the surface of the object can be inferred by following the displacement of a square subset of pixels, defined in the reference (undeformed) image, through the images taken during the welding. This procedure can be repeated for several subsets in the image, yielding for every pixel in the reference image, the displacement in all the deformed images. Further details of the method can be found in Sutton et al. [2].
In the experiment, spatial deformations are measured on a three-dimensional object. Therefore two cameras are setup, focussed on the side of the tube, see Fig.1.
At one side of the tube, in an area of about 40mm by 200mm the speckle pattern is applied. Markers (black crosses) are integrated in this speckle pattern as a reference for the focus of the cameras. These markers are also used in the processing of the images for assigning a coordinate system and for defining the position where the strain is extracted.
2400 images are taken to follow the strain evolution in the tube during the welding: in the first 600s two images per second and in the following 1200s one image per second.
The calculation of the DIC displacements and strains was performed with the Vic3D software from Correlated Solutions. In view of the smooth deformations in the application under investigation, the subset deformation is restricted to an affine transformation during the analysis. As the displacement of the subset from one image to the other may be smaller than one pixel, the subset in the deformed image is not likely to fit on the pixel grid and an interpolation method between the pixels is needed. Previous research [3,4] has shown that the approximate normalised sum of squared difference (NSSD) correlation algorithm reduces the systematic errors in the correlation process.
Next, the obtained displacements are smoothed via a so-called strain window method to reduce the impact of uncertainties and noise. This is a commonly adopted technique during the process of strain derivation [3]. In this step of the analysis, a plane is fit through the displacement values in the points around the centre of the strain window where displacements are available. This analytical approximation makes the calculation of the full-field strain information straightforward. In this research a default strain window of 5 is used. This means that the displacement field is smoothed over an area of 5px × 5px. As one pixel has a dimension of about 0.05 mm in the current images

and the measuring grid of the strain gauge is 3 × 6mm², the strain obtained from a strain gauge is in fact the average strain over this area, or speaking in terms of DIC, the strain averaged over a surface area of about 60px × 120px. To compare the strains obtained with DIC and those with a strain gauge, strains calculated with DIC presented here are averaged over an area of 3 × 6mm². The resulting strain evolution during the welding and the cooling of the tube in an area corresponding to respectively the strain gauge in the hoop and longitudinal directions, is plotted in Fig.3(a) and (b). A good overlap with the strain gauge measurements is obtained.

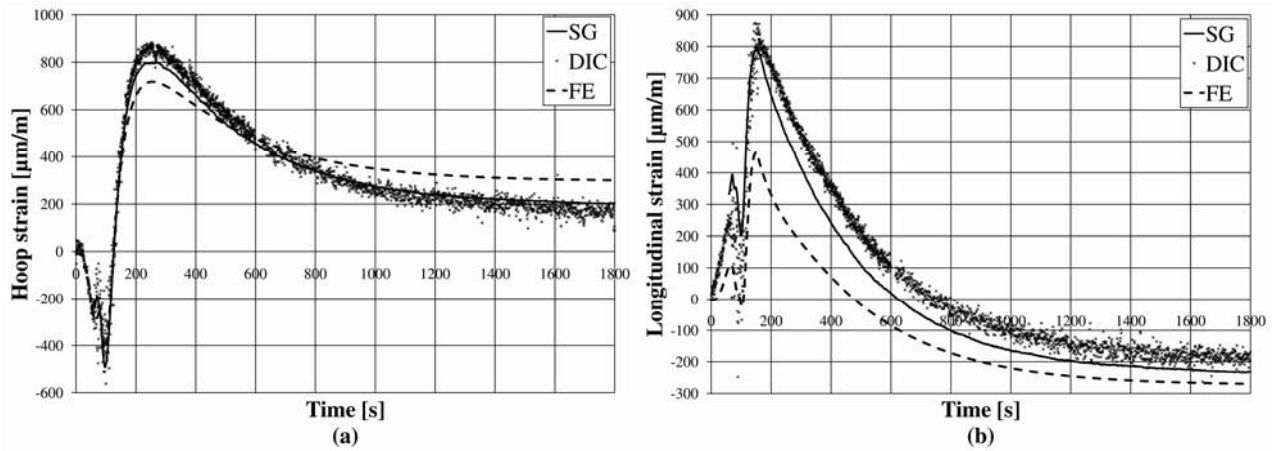

Fig.3. Comparison of strain gauge (SG), DIC and simulation (FE) results: (a) strain in hoop direction, for DIC and SG averaged over a zone corresponding to the strain gauge aligned in hoop direction and (b) longitudinal strain, for DIC and SG averaged over a zone corresponding to the strain gauge aligned in longitudinal direction.

2 FEA MODEL

The welding process is numerically simulated with the implicit code Abaqus/Standard. As is usual in welding simulations, the analysis is split up into two simulations, first the temperature field is calculated and then, based on the calculated temperatures, the thermal strain field is calculated. The symmetry in the problem is used in the FE model. For both analyses, the mesh is exactly the same and consists of quadrilateral shell elements. The elements are in axial direction 1mm long; in the weld they are about 0.5mm wide and on the opposite side 4.3mm wide.

2.1 Thermal model

In the thermal model, elements with five temperatures per node through the thickness are used. The parameters in the thermal model having the most influence on the result are: the heat input, the convection coefficient and the emissivity.
The power that is generated in the welding beam is defined as

$$Q = \eta \, . \, V \, . \, I$$

The voltage over the beam (V) is measured in the experiments and found to be 8V, the current through the beam (I) is in this welding process set to 38A. The efficiency (η) of the welding process indicates how much of the generated heat reaches the welded material. The heat input is distributed over the welded zone with the double ellipsoid as defined by Goldak [5]. This heat distribution model is implemented in the simulations with a user subroutine DFLUX.
The emissivity was measured experimentally and found to be 0.15. The values for η and the convection coefficient are based on a Levenberg-Marquardt optimization method which minimizes the difference between the temperature curves measured with the five thermocouples in the experiment and those calculated in the corresponding positions in the FE model.
Other temperature-dependent, thermal material properties (density, conductivity, heat capacity) are taken from literature [6-8]: for the density a value of 7850kg/m³ is taken, the value for the thermal conductivity is increasing from about 15W/m/K at room temperature to a value of about 30W/m/K at 1200°C; the specific heat c_a (J/kg/K) is determined in function of the actual temperature (T) as:

$$c_a = 450 + 0.28 \,.\, T - 2.91 \,.\, 10^{-4} \,.\, T^2 + 1.34 \,.\, 10^{-7} \,.\, T^3$$

In this way the simulated temperature field should be in fair agreement with the experimentally measured one.

2.2 Mechanical analysis

The temperatures in each node are used as input for the mechanical analysis. Linear elements with reduced integration (one integration point) are used. As the thermal expansion of the material is the driving force behind the origin of stresses and strain when a construction is welded, the thermal expansion coefficient of the RVS304 material, used in these experiments, was measured in a separate series of experiments [9]. The inferred behaviour of the thermal expansion is presented in Fig.4(a). The stiffness of the material reduces with rising temperature. The Young's modulus adopted in the model is given in Fig.3(a) and was taken from Gardner et al. [6]. The plastic behaviour of the material at room temperature was obtained from tensile tests on tubular material. The behaviour at higher temperatures was obtained by applying the reduction factors of Chen et al. [10] on the room temperature data. The resulting material model is given in Fig.4 (b). In the plastic region, the material is assumed to satisfy the von Mises yield criterion combined with isotropic hardening. All the material parameters are supposed to behave isotropically.

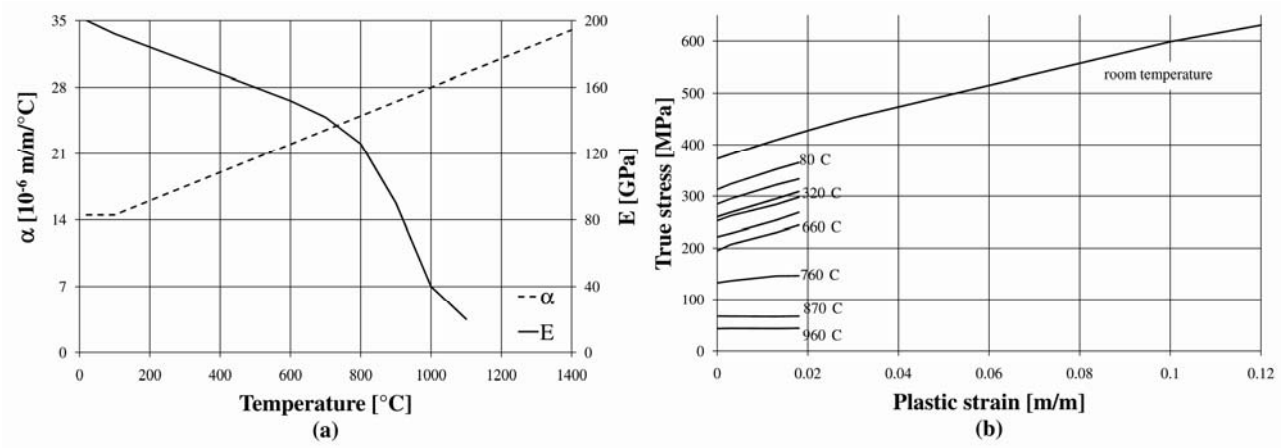

Fig.4. Input for the mechanical analysis: (a) thermal expansion coefficient α and Young's modulus E [6] in function of temperature and (b) plastic material behaviour in function of temperature.

The results of the FE simulations are given in Fig.3. Here also the strains are averaged over an area corresponding to a strain gauge. For the FEA, the area of 3 × 6mm² corresponds with eight elements. Strains are extracted for the outer surface of the shell elements.

3 DISCUSSION

3.1 Strain gauges and DIC

When looking at the results in Fig.2, the strain gauge and temperature results are apparently not available for the first few seconds. This is because when the weld beam is started, the sensors are not connected to the amplifier to avoid problems with electrical fields that accompany the starting of the weld beam. Also noticeable is that at time=1800s, the compensated and the uncompensated strain are not coinciding. This is because the tube cannot completely cool down to the reference state of the strain gauge measurement. For the DIC measurement, additional illumination with a halogen spotlight is necessary, and this raises the temperature around the setup with about 5°C. The reference state for the strain gauge measurement is before additional illumination.

The reference state for the DIC measurement is with additional illumination (otherwise it is not possible to make images). This different reference state in the two experimental methods is taken into account in the compensated strain gauge curve.

The DIC strain evolution is noisier than the strain gauge curve obtained from the strain gauges. They yield very similar results, both qualitatively and quantitatively, for both strain components as can be seen in Fig.3. Based on these results it can be justified to rely on DIC results, which are available in a region of 80 × 20mm² on the surface of the tube.

3.2 Comparison experimental and numerical results

The strain evolution calculated with FEA shows good agreement if the hoop strain is compared to the DIC result. For the longitudinal strain, only qualitative correspondence is found: the curve of the strain evolution has the same shape: peaks occur at the same time and in the same direction, but their values are certainly not in agreement. From these results it is clear that in the mechanical analysis some model input parameters should be estimated more accurately. It is however positive that there is qualitative agreement between simulation and experiment, taking into account the complexity of estimating the temperature dependency of the thermomechanical material parameters needed in these models.
It should be mentioned that the validation of the thermal simulation is based on only five points in the tube. An additional validation of this simulation can be done by also checking the geometry of the melt pool.

4 CONCLUSION

From the results presented in this contribution it is concluded that the measured strain evolution can be trusted: strain gauges and DIC yield similar strain evolution during the welding.
When the strain evolution of the finite element simulation is compared to the experimental results, it is clear that they are qualitatively in agreement. A similar shape is found and peaks occur at the same point in time. This agreement is also quantitatively for the strain in hoop direction, in longitudinal direction, however, the values of the strains are not in agreement. Future work will consist of optimizing the input of the FEA model.

REFERENCES

[1] Lindgren, LE, “Finite element modeling and simulation of welding part 3: efficiency and integration”, Journal of Thermal Stresses, Vol. 24, pp. 305–334, 2001.

[2] Sutton, MA, Orteu, JJ, and Schreier, H.W, *Image Correlation for Shape, Motion and Deformation Measurements*, Springer, New York, 2009.

[3] Lava, P, Cooreman, S, Coppieters, S, De Strycker, M and Debruyne, D, “Assesment of measuring errors in DIC using deformation fields generated by plastic FEA”, Optics and Lasers in Engineering, Vol.47, pp.747–753, 2009.

[4] Schreier, HW, Braasch, JR, and Sutton, MA, “Systematic errors in digital image correlation caused by intensity interpolation”, Optical Engineering, Vol. 39, pp. 2915–2921, 2000.

[5] Goldak, JA, Akhlaghi, M, *Computational welding mechanics*, Springer, New York, 2005.

[6] Gardner, L and Baddoo, NR, “Fire testing and design of stainless steel structures”, Journal of Constructional Steel Research, Vol. 62, pp. 532–543, 2006.

[7] Gardner, L and Ng, KT, “Temperature development in structural stainless steel sections exposed to fire”, Fire Safety Journal, Vol. 41, pp. 185–203, 2006.

[8] Mahin, KW, Winters, W, Holden, TM, Hosbons, RR and MacEwen, SR, “Prediction and measurement of residual elastic strain distributions in gas tungsten arc welds”, Welding Journal, Vol. 70, pp. 245s–260s, 1991.

[9] De Strycker, M, Schueremans, L, Van Paepegem, W, and Debruyne, D, “Measuring the thermal expansion coefficient of tubular steel specimens with digital image correlation techniques”, Optics and Lasers in Engineering, Vol. 48, pp. 978–986, 2010.

[10] Chen, J and Young, B, “Stress-strain curves for stainless steel at elevated temperatures”, Engineering Structures, Vol. 28, pp. 229–239, 2006.